Liquid-Column Sustainment Driven by Acoustic Wave Guiding

Nicolas Bertin, Régis Wunenburger,* Etienne Brasselet, and Jean-Pierre Delville

Centre de Physique Moléculaire Optique et Hertzienne, UMR CNRS 5798, Université Bordeaux I, 351 cours de la Libération, 33405 Talence Cedex, France

(Received 12 February 2010; published 11 October 2010)

We report on the formation and sustainment of liquid columns with aspect ratios much larger than the value at the onset of the Rayleigh-Plateau instability. This is achieved by using the passive feedback of the radiation pressure applied on the column surface by an acoustic beam injected at the upper end of the column and guided along it. We develop an analytical model that describes the coupling between the acoustic wave guiding and the balance between acoustic and capillary surface forces exerted on the column surface and find a satisfactory agreement with the experiment.

DOI: 10.1103/PhysRevLett.105.164501 PACS numbers: 47.20.Dr, 43.25.+y, 47.20.Gv, 47.55.nk

The control of the geometry and stability of liquid columns is of paramount importance in many processes implemented at scales ranging from macroscopic to nanometric, such as float-zone crystal growth [1], liquid jet polishing of optics [2], wire and fiber coating [3], protein microarray fabrication [4], or nanolithography [5]. The long term sustainment of liquid columns with large and controllable aspect ratios is naturally challenging on account of interfacial energy minimization [6]. A well-known example is the cylindrical liquid bridge with fixed ends and volume, that breaks into droplets through the Rayleigh-Plateau (RP) instability when its aspect ratio $\Lambda = L/2R$ exceeds π in weightless conditions, L and R being the length of the liquid column and the radius of its circular cross section, respectively [6].

Since the pioneering attempts to stabilize liquid columns using a static axial electric field by Raco [7] and Taylor [8], several passive [9–11] and active [12–14] strategies have been implemented in order to push further the onset of the RP instability. Nevertheless, none of the recently developed stabilization techniques based on the application of an external field—be it electric [9,10,13–15] or acoustic [11,12]—succeeded in stabilizing columns made of simple liquids of aspect ratios larger than 5.2. However, the maximum aspect ratio $\Lambda_{\max}$ attainable using passive feedback theoretically increases with the field intensity and is thus *a priori* not limited. The questions of whether and how liquid columns of larger aspect ratios can be sustained thus remain open and challenging problems.

Up to now, acoustic stabilization has been achieved by locating the liquid column at a radiation pressure node of a standing wave whose direction is perpendicular to the column [11,12]. Such a geometry, however, makes the stabilization process very sensitive to the details of the actual acoustic field surrounding the liquid column and, more importantly, breaks its axial symmetry [11]. On the other hand, very recently, bulk [16] and surface [17] acoustic waves have been shown to be able to trigger interface destabilization leading to jetting, whereas amplitude modulated leaky waves propagating along liquid jets have been used to control jet breakup [18]. In this Letter, we experimentally demonstrate that acoustic wave guiding by the liquid column itself, which preserves its axial symmetry, can be efficiently used to *stabilize* it. We indeed report on the formation and sustainment of liquid columns made of standard Silicone oil within a water bath with aspect ratios much larger than its value at the onset of the RP instability and even larger than any values formerly reached. To achieve this, we exploit the passive feedback of the acoustic radiation pressure applied by an ultrasonic beam injected at the upper end of the liquid column and guided along it. We propose an analytical model that describes the coupling between the acoustic guiding and the balance of acoustic and capillary surface forces exerted on the column surface and find a satisfactory agreement with the measured column radii. Moreover, the observed robustness of this stabilization technique is explained by performing a linear stability analysis of the liquid column.

Experiment.—A spherical ultrasonic transducer (focal length 38 mm, diameter 38 mm, central frequency $f = \omega/2\pi = 2.25$ MHz, bandwidth 600 kHz) is immersed vertically in a 40 mm thick layer of 20 cSt kinematic viscosity Silicone oil (upper oil reservoir) covering a 150 mm thick layer of pure water, both contained in an open transparent tank, see Fig. 1(a). A sessile Silicone oil droplet, of 20 mm typical diameter, is placed at the bottom of the water layer. The droplet, whose volume is controlled by a syringe located outside the tank, plays the role of the lower reservoir. The droplet sits on a sheet of acoustic absorber lying on a moving pad. The transducer is supplied by a power amplifier driven by a waveform generator that periodically emits at $f' = 20$ kHz repetition rate sinusoidal wave trains at carrier frequency f, of 22 periods duration and of peak-to-peak voltage U.

In order to form a liquid column, the initially horizontal oil-water interface is first positioned above the focus at an altitude z_{init} ranging from -3.5 mm to -5 mm [here (r, θ, z) are cylindrical coordinates centered on the

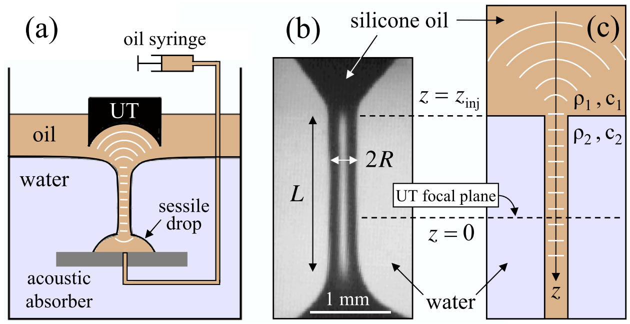

FIG. 1 (color online). (a) Sketch of the experimental setup. UT: focused ultrasonic transducer. (b) Acoustically stabilized liquid column of aspect ratio $\Lambda = 6.2$ using a UT driving voltage amplitude $U = 25.5$ V (altitude of the initially flat interface $z_{\rm init} = -5$ mm). (c) Geometry of the model.

transducer symmetry axis and of origin the transducer focus, see Fig. 1(c)]. Then U is increased and fixed beyond the threshold of formation of an oil-in-water dripping jet by the radiation pressure of the incident acoustic beam [16]. Then, by raising the pad, the jet tip is brought into contact and coalesces with the sessile drop, thus forming a vertical liquid column with small aspect ratio between both oil reservoirs. Finally, the pad is stepwise brought down until the column breaks up. The radius profile $R(z)$ of the longest steady column is then extracted by video postprocessing, see Fig. 2(a). $R(z)$ exhibits a wide plateau whatever U which allows us to define the column radius R as the average of $R(z)$ over the plateau defined from $R(z)$ histograms.

In absence of flow, the equilibrium shape of a column is determined by the balance of the capillary stresses due to the interfacial tension γ, the hydrostatic pressure imbalance between both liquids and the acoustic radiation normal stress Π usually called radiation pressure. Labeling 1 (2) the oil (water) phase, the interfacial stress balance equation is written $p_{1,0} - p_{2,0} + (\rho_1 - \rho_2)g(z - z_{\rm init}) + \Pi[R(z)] = \gamma\kappa[R(z)]$, where $\gamma = 0.033\ {\rm N\,m^{-1}}$, $\rho_1 = 950\ {\rm kg\,m^{-3}}$ ($\rho_2 = 1000\ {\rm kg\,m^{-3}}$) is oil (water) density, $p_{i,0}$ is the pressure at the interface in fluid $i = 1, 2$ at $z = z_{\rm init}$, g is Earth's gravitational acceleration, $\kappa = (1 + (\partial_z R)^2)^{-1/2}(R^{-1} - \partial_{zz}R)$ is the interface curvature assuming the column to be axially symmetric, and $\gamma\kappa$ the Laplace pressure. Since far away from the acoustic beam the interface is located at $z = z_{\rm init}$ and is flat [see Fig. 1(a)], $p_{1,0} = p_{2,0}$. On the other hand, the Bond number ${\rm Bo} = g(\rho_2 - \rho_1)R^2/\gamma$ associated to the column is of the order of 6×10^{-4} so that gravity effects can be safely neglected [19]. Consequently Π solely determines the column shape at equilibrium,

$$\Pi[R(z)] = \gamma\kappa[R(z)]. \qquad (1)$$

The right-hand side of Eq. (1) can be experimentally assessed from $R(z)$, as shown in Fig. 2(b). We observe a plateau that demonstrates the invariance of the acoustic radiation pressure along the stabilized column over distances of the order of, or larger than, the natural diffraction length of the acoustic beam, equal to 1.6 mm. This indicates that

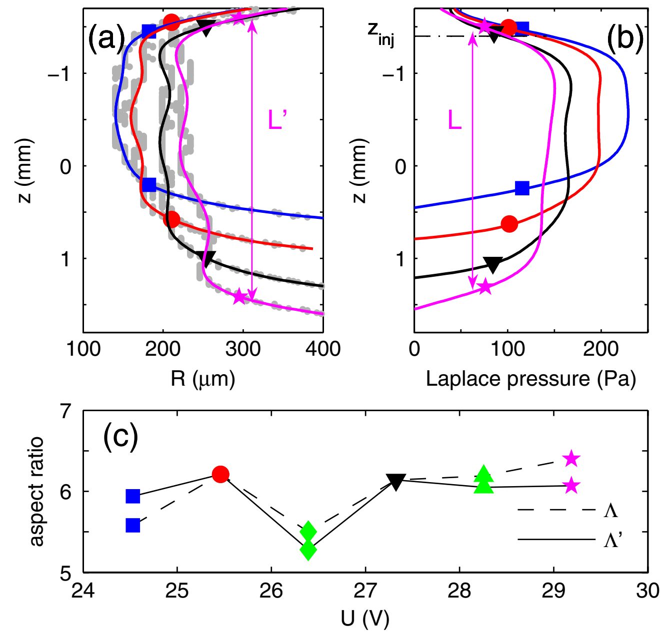

FIG. 2 (color online). (a) Radius profiles $R(z)$ of acoustically stabilized liquid columns of optimal length for various values of U [see (c) for curve identification] and for $z_{\rm init} = -5$ mm. Dots: digitized column profiles; solid curves: 10th degree polynomial fits. The column radius R is defined as the average of $R(z)$ over the plateau. Pairs of symbols indicate the full width at 125% of R defining the length L'. (b) Corresponding altitude dependent Laplace pressure $\gamma\kappa$ [see (c) for curve identification]. Pairs of symbols indicate FWHM defining the length L. (c) Solid curve: aspect ratio $\Lambda = L/2R$ as function of U. Dotted curve: $\Lambda' = L'/2R$. Symbols label the curves shown in (a) and (b).

the beam is guided by the liquid column. This is consistent with the sound speed values $c_1 = 998\ {\rm m\,s^{-1}} < c_2 = 1488\ {\rm m\,s^{-1}}$ in the column and the outer bath, respectively, ensuring the total internal reflection condition to be satisfied.

From the latter considerations we introduce the column length L as the length of its part exhibiting a constant Laplace pressure. More precisely, since in both reservoirs $\gamma\kappa$ is expected to tend toward values much smaller than its maximum, we define L as the full width at half maximum (FWHM) of $\gamma\kappa(z)$, see Fig. 2(b). The dependence of $\Lambda = L/2R$ versus U is shown in Fig. 2(c). We observe that Λ does not significantly depend on U and is reproducibly much larger than π. On the other hand, we define the bridge length L' as the length of its portion satisfying $R(z) = R \pm \Delta R$, where $\Delta R/R = 25\%$ is the typical amplitude of observed bridge radius fluctuations in former experiments on passive acoustic stabilization of liquid bridges [11]. We find that $\Lambda' = L'/2R$ exhibits values comparable to Λ, as shown in Fig. 2(c). Importantly, we note that the column volume is not fixed by our setup and the volume of both oil reservoirs is much larger than the volume of the column. So, considering the response of the column to any shape perturbation, both oil reservoirs should behave as constant pressure tanks. Consequently, the constraint applied on the perturbation is rather a fixed pressure than a fixed volume constraint and the predicted aspect ratio at the instability threshold is not π but $\pi/2$ [6]. The stabilization mechanism is thus even more efficient than estimated at first sight. Now, in order to get more insight into the stabilization mechanism, we first model the beam injection into the liquid column and the acoustic wave guiding along it. Then the acoustic radiation stresses acting on the column surface are calculated and the column equilibrium radius as well as its stability are determined.

Model.—Assuming the acoustic propagation as nondissipative, we can write the fluid velocity $\mathbf{u}$ as $\mathbf{u} = \boldsymbol{\nabla}\psi$, where ψ is the velocity potential, and the fluid pressure fluctuation around its hydrostatic value p as $p = -\rho\partial_t\psi$. Considering the acoustic propagation as linear and a harmonic excitation of the transducer, the acoustic field is assumed to be harmonic with pulsation ω, and its propagation is conveniently described using complex notation. An accurate description of the incident beam near the upper end of the liquid column, i.e., upstream from the focus [see Fig. 2(a)] is required to model the beam injection. We thus have measured the modulus and phase of the incident pressure field $p_\omega^{(\mathrm{inc})}(r, z) \propto U$ produced in Silicone oil by the transducer driven sinusoidally at small U using a 40 μm diameter active element hydrophone and a lock-in amplifier. We found that a paraxial integral model of the field of a focused transducer [20] accurately fits these pressure measurements (not shown here). The pressure measurements and the paraxial integral model are independently fitted at each z by a Gaussian beam model with waist w_0 and offset z^* for $r \leq 400$ μm $p_\omega^{(\mathrm{inc})}(r, z) \propto \frac{w_0}{w} e^{-(r^2/w^2)} \exp\{j[\frac{k_1 r^2}{2\mathcal{R}} + k_1 z^* - \arctan(\frac{z^*}{z_0})]\}$ where $z_0 = \pi w_0^2 f/c_1$ is the beam diffraction length, $\mathcal{R} = -z^*(1 + z_0^2/z^{*2})$ the wave front radius of curvature along the axis at z^* and $w = w_0(1 + z^{*2}/z_0^2)^{1/2}$ the beam diameter at z^*. Figure 3(a) displays the z dependence of the parameters w_0 and z^* of the Gaussian representation of the pressure field. In order to achieve a full analytical description, such a Gaussian representation will be used instead of the paraxial integral model.

The injection of the incident beam into the liquid column through its funnel-shaped upper end [see Fig. 1(b)] is modeled by considering a sharp end [see Fig. 1(c)] located at altitude z_{inj} that is the only free parameter of the model. We assume a piecewise transmission at z_{inj} of the incident beam as a plane wave of potential $\psi_{1,2}^{(\mathrm{inj})}$, i.e. $\psi_1^{(\mathrm{inj})}(r, z_{\mathrm{inj}}) = \psi^{(\mathrm{inc})}(r, z_{\mathrm{inj}})$ for $0 \leq r \leq R$ and $p_2^{(\mathrm{inj})}(r, z_{\mathrm{inj}}) = T_p p^{(\mathrm{inc})}(r, z_{\mathrm{inj}})$, $u_{z,2}^{(\mathrm{inj})}(r, z_{\mathrm{inj}}) = T_u u_z^{(\mathrm{inc})}(r, z_{\mathrm{inj}})$ for $r \geq R$, where $T_p = 2Z_1/(Z_1 + Z_2)$ and $T_u = 2Z_2/(Z_1 + Z_2)$ are the pressure and velocity transmission coefficients, respectively, with $Z_i = \rho_i c_i$ the acoustic impedance of fluid i, $i = 1, 2$.

Then, we describe the guiding of the incident beam along the liquid column as the superposition of the guided, propagating, θ invariant modes associated to an infinitely long cylindrical waveguide of radius R. The velocity potential of these modes labeled by integer m satisfies the pressure and radial velocity continuity at the column surface and writes $\psi^{(m)}(r) = \psi_0^{(m)} e^{j(\omega t - \beta_m z)} F^{(m)}(r)$, where $\psi_0^{(m)}$ is a constant, $F^{(m)}(r) = \frac{J_0(\kappa_m r)}{J_0(\kappa_m R)}$ if $r \leq R$ and $F^{(m)}(r) = \frac{\rho_1}{\rho_2}\frac{K_0(\gamma_m r)}{K_0(\gamma_m R)}$ if $r \geq R$, J_0 (K_0) being the zeroth order Bessel function of the first (second) kind [21]. κ_m and γ_m are defined as $\kappa_m = [(\omega/c_1)^2 - \beta_m^2]^{1/2}$ and $\gamma_m = [\beta_m^2 - (\omega/c_2)^2]^{1/2}$, β_m being the mth smallest root of the dispersion equation $\kappa_m J_1(\kappa_m R)/J_0(\kappa_m R) = \gamma_m \frac{\rho_1}{\rho_2} K_1(\gamma_m R)/K_0(\gamma_m R)$. Its numerical resolution shows that it has a single root labeled by $m = 1$ for $R \leq 350$ μm. Therefore the observed liquid columns behave as monomodal acoustic waveguides. In order to determine the amplitude of the propagating acoustic field guided along the column labeled as g, we use the Hermitian product defined as $\langle\psi_\alpha\psi_\beta\rangle = \int_0^\infty \frac{1}{2}(p_\alpha u_{z,\beta}^* + p_\beta^* u_{z,\alpha}) 2\pi r dr$ that satisfies the acoustic energy flux conservation and for which the guided propagating and leaky modes together with the radiating modes constitute an orthogonal basis. Its velocity potential writes $\psi^{(g)} = a_1\psi^{(1)}$, where

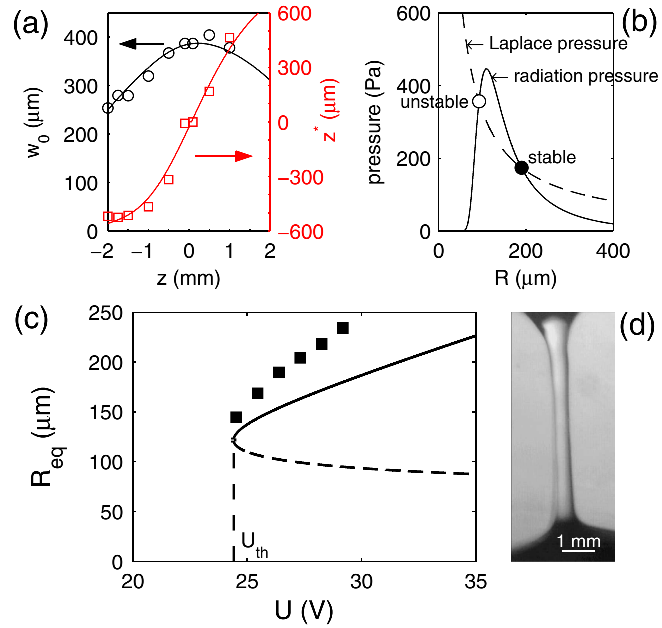

FIG. 3 (color online). (a) z dependence of effective waist w_0 (black) and offset z^* (red) of the Gaussian beam representation of the measured incident pressure field $p_\omega^{(\mathrm{inc})}(r, z)$ (symbols) and of the paraxial integral model (solid curves, see text). (b) Dashed (solid) curve: R dependence of the Laplace pressure $\gamma\kappa$ (radiation pressure Π computed for $U = 30$ V and using for z_{inj} its best fit value -1.4 mm). Open (filled) circle: unstable (stable) uniform solution of Eq. (1). (c) Symbols: measured liquid-column radii versus transducer voltage U. Solid (dotted) curve: predicted stable (unstable) column radius $R_{\mathrm{eq}}(U)$ using $z_{\mathrm{inj}} = -1.4$ mm. (d) A $\Lambda \simeq 11$ stable liquid column, however, nonreproducibly observed.

$a_1 = \frac{\langle \psi^{(\mathrm{inj})} \psi^{(1)} \rangle}{\langle \psi^{(1)} \psi^{(1)} \rangle}$ is computed using the Gaussian beam representation of the incident beam.

Next, we assume the stress exerted on the liquid column of radius R to be due to the propagating, guided acoustic field of potential $\psi^{(g)}$ only. According to Brillouin [22], the time averaged acoustic radiation stress tensor $\mathbb{S}_i$ in fluid i is $\mathbb{S}_i = (\frac{\rho_i}{2} \langle \mathbf{u}_i^{(g)2} \rangle_t - (2\rho_i c_i^2)^{-1} \langle p_i^{(g)2} \rangle_t) \mathbb{I} - \rho_i \langle \mathbf{u}_i^{(g)T} \mathbf{u}_i^{(g)} \rangle_t$, where $\mathbb{I}$ is the identity tensor, ${}^T\mathbf{u}$ the transpose of $\mathbf{u}$ and $\langle \cdots \rangle_t$ denotes time averaging. The resulting interfacial stress $\mathbf{\Pi} = (\mathbb{S}_2 - \mathbb{S}_1)_{r=R} \cdot \mathbf{e}_r$ is purely radial. Since wave trains are used, we assume the liquid column to respond only to the time averaged mechanical effects of the acoustic field. The repetition period $1/f'$ is indeed much smaller than the characteristic time scale $\tau \sim \eta_1 R/\gamma \simeq 0.13$ ms of the viscous dynamics of the column (η_1 is the dynamic viscosity of fluid 1). We also assume the models of acoustic propagation and of their associated mechanical effects established for a continuous, harmonic excitation, to be also valid for wave trains carrying the same time averaged acoustic energy. Therefore we simply multiply U by the square root of the experimental duty cycle fraction $(22f'/f)^{1/2}$. The resulting R dependence of Π is shown in Fig. 3(b) for $U = 30$ V.

Finally, for a given value of U, the predicted liquid-column radius R_{eq} is the constant solution of Eq. (1), $\Pi(R_{\mathrm{eq}}) = \gamma/R_{\mathrm{eq}}$, satisfying the mechanical stability criterium $\partial\Pi/\partial R|_U(R_{\mathrm{eq}}) < \partial(\gamma/R)/\partial R|_U(R_{\mathrm{eq}})$, as illustrated in Fig. 3(b). Since liquid-column stabilization is predicted to occur only above a threshold voltage U_{th}, in agreement with experiments, the value -1.4 mm is chosen for z_{inj} so as to make both U_{th} and the experimental threshold voltage coincide. We note from Fig. 2(b) that this altitude corresponds with the beginning of the plateau of Laplace pressure, i.e., of z invariant wave guiding, for all the observed columns. This self-consistently validates our sharp column end model of beam injection. Moreover, as shown in Fig. 3(c), the predicted values of column radius are in satisfactory agreement with the measured ones. The remaining discrepancy may be mainly ascribed to the contribution of nonguided modes to the radiation pressure and to the effect of acoustic streaming.

Discussion.—An insight into the robustness of the acoustic stabilization can be grasped from the linear stability analysis of the liquid column following [11]. We consider infinitesimal sinusoidal disturbances with wave number K of the column radius, δR, and pressure of the inner fluid, δp_1. Then we assume an adiabatic variation of the guided acoustic field along the perturbed column. The linearization of the interfacial stress balance equation around the column equilibrium state reads: $\delta p_1 = C(K)\delta R$ with $C(K) = -\gamma/R_{\mathrm{eq}}^2 - \partial\Pi/\partial R|_U(R_{\mathrm{eq}}) + \gamma K^2$. Since (i) overall stability (i.e., release of any bulge through pressure difference induced axial flow) is achieved when $C(K) > 0\ \forall\ K$, (ii) the condition of column stabilization is $C(0) > 0$, and (iii) $C(K) \geq C(0)\ \forall\ K$, a liquid column is found to be stable against perturbations of any wave number. Consequently, liquid columns of any aspect ratio could theoretically be stabilized with our technique. This explains why liquid columns of very large aspect ratios like the one shown in Fig. 3(d) were observed, although nonreproducibly.

To conclude, we implemented and described a new strategy to stabilize liquid columns of large aspect ratios based on the passive feedback of the radiation pressure applied by an acoustic beam guided along the column. We emphasize that the obtained stability results from the perfect balance between the Laplace pressure and the z-invariant acoustic stress resulting from wave guiding. This distinguishes our approach from former passive stabilization strategies [9–11]. We finally note that, although strictly speaking guiding is not achievable in the case of a liquid column in air, the large impedance mismatch between the column and the air may result in an almost invariance of the acoustic field along the liquid column, enabling to implement our technique in this case too.

*Corresponding author: r.wunenburger@cpmoh.u-bordeaux1.fr

[1] J. Meseguer *et al.*, Current Topics in Crystal Growth Research **5**, 27 (1999).
[2] A. B. Shorey, D. Golini, and W. Kordonski, Opt. Photonics News **18**, No. 10, 14 (2007).
[3] D. Quéré, Annu. Rev. Fluid Mech. **31**, 347 (1999).
[4] M. Hartmann *et al.*, Anal. Bioanal. Chem. **393**, 591 (2009).
[5] E. Schäffer *et al.*, Nature (London) **403**, 874 (2000).
[6] B. J. Lowry and P. H. Steen, Proc. R. Soc. A **449**, 411 (1995).
[7] R. J. Raco, Science **160**, 311 (1968).
[8] G. Taylor, Proc. R. Soc. A **313**, 453 (1969).
[9] H. Gonzalez *et al.*, J. Fluid Mech. **206**, 545 (1989).
[10] S. Sankaran and D. A. Saville, Phys. Fluids A **5**, 1081 (1993).
[11] M. J. Marr-Lyon, D. B. Thiessen, and P. L. Marston, Phys. Rev. Lett. **86**, 2293 (2001).
[12] M. J. Marr-Lyon, D. B. Thiessen, and P. L. Marston, J. Fluid Mech. **351**, 345 (1997).
[13] M. J. Marr-Lyon *et al.*, Phys. Fluids **12**, 986 (2000).
[14] D. B. Thiessen, M. J. Marr-Lyon and P. L. Marston, J. Fluid Mech. **457**, 285 (2002).
[15] A. Ramos, H. Gonzalez, and A. Castellanos, Phys. Fluids **6**, 3206 (1994).
[16] B. Issenmann *et al.*, Europhys. Lett. **83**, 34 002 (2008).
[17] M. K. Tan, J. R. Friend, and L. Y. Yeo, Phys. Rev. Lett. **103**, 024501 (2009).
[18] J. B. Lonzaga *et al.*, J. Acoust. Soc. Am. **121**, 3323 (2007).
[19] S. R. Corriell, S. C. Hardy, and M. R. Cordes, J. Colloid Interface Sci. **60**, 126 (1977).
[20] G. S. Kino, *Acoustic Waves, Devices, Imaging and Analog Signal Processing* (Prentice-Hall, Englewood Cliffs, NJ, 1987), p. 184.
[21] W. J. Jacobi, J. Acoust. Soc. Am. **21**, 120 (1949).
[22] L. Brillouin, Ann. Phys. (Paris) **4**, 528 (1925).